94 年水資源管理研討會

不飽和邊坡之降雨入滲模擬
A Simulation of Rainfall Infiltration for an Unsaturated Slope

馮正一 (通訊作者)
國立中興大學 水土保持學系 助理教授
402 台中市國光路 250 號
行動: 0928589110
傳真: 886-4-22876851
E-mail: tonyfeng@dragon.nchu.edu.tw

張育瑄
國立中興大學 水土保持學系 研究生
402 台中市國光路 250 號
行動: 0928779357
E-mail: rainboy7492@yahoo.com.tw

不飽和邊坡之降雨入滲模擬

A Simulation of Rainfall Infiltration for an Unsaturated Slope

國立中興大學水土保持學系
助理教授
馮正一
Zheng-yi Feng*

國立中興大學水土保持學系
研究生
張育瑄
Yu-hsuan Chang

摘要

本研究選擇了在 1999 年發生集集地震時有大規模崩塌的九份二山之不飽和土壤滲透試驗資料，利用有限差分程式(FLAC 5.0)進行邊坡降雨入滲的不飽和土壤水份傳輸模擬與降雨入滲後邊坡穩定安全係數之變化。數值模擬的結果顯示，邊坡有沖蝕控制的處理會減小位移及增加邊坡的穩定度。由模擬結果亦可發現在邊坡降雨入滲的速度不快，在不飽和土壤水流動很慢的所以入滲對邊坡的影響並不大。因此，如果對較陡地區做好沖蝕控制，單只有入滲較不可能引起邊坡破壞。

關鍵詞:不飽和土壤、降雨入滲、邊坡穩定

Abstract

A large landslide site, Jiu-fen-er-shan, caused by Chi-chi earthquake in 1999, is selected for the numerical simulations using the finite difference code (FLAC 5.0) for the effects of infiltration on slope using the rainfall event during a typhoon. The numerical results show that displacement will be smaller and stability will be higher for a slope treated with erosion control. It is also shown that rainfall infiltration into slope is slow and the effect could be small due to the nature of slow water transport in unsaturated soil. Therefore, if a landslide prone area has been treated with erosion control, infiltration alone is unlikely to trigger a slope failure.

Keyword: unsaturated soil, rainfall infiltration, slope stability

1. Introduction

The Chi-Chi earthquake (M_L=7.3) struck Taiwan in September 21, 1999 and caused an 80 km surface rupture, the Chelunpu fault. The horizontal acceleration was measured as high as one gravity (980 gal) with strong vertical shaking. This caused numerous landslides in central Taiwan and remained many fractured slopes. In addition, Taiwan is located in the path of tropical typhoons which bring tremendous rainfalls almost every year during summer. The averaged annual rainfall of the world is about 500mm. However, the averaged rainfall in Taiwan is from

2500 to 3000mm annually. Therefore, after the earthquake and typhoons during summer, many of the mountain slopes were remained unstable and easy to slide.

Rainfalls infiltrating into slope may cause stability problem of a slope. A numerical procedure is proposed in this study to study the effects of infiltration on slope. Experimental result for unsaturated flow parameters of Jiu-fen-er-shan is selected as the example input of the numerical analysis. For numerical simulations of the infiltration, a rainfall record during Typhoon Mindulle was used and FLAC code was adopted for the analyses. Numerical results showed that the displacement will be smaller and stability will be improved for a slope treated with the erosion control method.

2. Theoretical Background of the Unsaturated Flow Simulation

FLAC 5.0 (FLAC, 2005) is an explicit finite difference code that is capable of simulating both saturated and unsaturated flow. Both saturated (wetting) and unsaturated (non-wetting) fluid transport in soil slopes can be described by Darcy's law as following:

$$q_i^w = -k_{ij}^w \kappa_r^w \frac{\partial}{\partial x_j}(P_w - \rho_w g_k x_k)$$

$$q_i^g = -k_{ij}^w \frac{\mu_w}{\mu_g} \kappa_r^g \frac{\partial}{\partial x_j}(P_g - \rho_g g_k x_k)$$

k_{ij}^w : saturated mobility coefficient

κ_r : relative permeability for the fluid

μ : dynamic viscosity

P : pore pressure

ρ : fluid density

g : gravity

subscript g : non - wetting fluid

subscript w : wetting fluid

Relative permeabilities are related to saturation, S_w, by empirical law of the van Genuchten (1980) as following:

$$\kappa_r^w = S_e^b \left[1 - \left(1 - S_e^{1/a}\right)^a\right]^2$$

$$\kappa_r^g = (1 - S_e)^c \left[1 - S_e^{1/a}\right]^{2a}$$

a, b, c : constant parameters

S_e : effective saturation

The effective saturation is defined as:

$$S_e = \frac{S_{w-} S_r^w}{1 - S_r^w}$$

S_r^w : residual wetting fluid saturation

We can combine the fluid balance laws with the fluid constitutive laws to the fluid balance equation as following (FLAC, 2005):

$$n\left[\frac{S_w}{K_w}\frac{\partial P_w}{\partial t} + \frac{\partial S_w}{\partial t}\right] = -\left[\frac{\partial q_i^w}{\partial x_i} + S_w \frac{\partial \varepsilon}{\partial t}\right]$$

$$n\left[\frac{S_g}{K_g}\frac{\partial P_g}{\partial t} + \frac{\partial S_g}{\partial t}\right] = -\left[\frac{\partial q_i^w}{\partial x_i} + S_g \frac{\partial \varepsilon}{\partial t}\right]$$

ε : volumetric strainnn

n : porosity

P : pore pressure

K : fluid bulk moduli

In a fluid-only calculation, the term $\frac{\partial \varepsilon}{\partial \mathrm{t}}$ is omitted. The fluid balance equations are solved in FLAC using a discretization and explicit finite-difference method.

3. Procedures and the Numerical Model for Rainfall infiltration

A numerical procedure is used to examine the effects of rainfall infiltration on slope using the, FLAC code. A fictitious slope is assumed for the simulations and is shown in FIGURE 1. For this slope, the finite difference mesh is created as shown in FIGURE 2.There are 3 points selected for numerical monitoring, Point 1 located at crest of the slope, Point 2 located at mid-slope, and Point 3 located at the toe of the slope. The procedures are listed as following:

- Initial steady state for groundwater seepage and initial negative pore pressures in the unsaturated zone above the groundwater table
- Perform mechanical static equilibrium
- Perform rainfall infiltration simulations for 36 hours using the rainfall records during typhoon
- Calculate factor of Safety (F.S.) calculations for every 12 hours

Additional numerical simulations are included to show the differences under different

assumptions. In this study, there are three numerical cases, “Case 1”, “Case 2” and “Case 3”. Case 1 represents crack filling treatment on slopes for the erosion control but without surface drainage system installed. Case 2 represents crack filling and surface drainage system installed. To simulate drainage pipes that is often installed at the toe of a slope, the “interior wells” can be setup near the toe of the slope in the numerical model with a discharge 0.00005 m^3/sec. This is the “Case 3” in this study. The rainfall input records are adopted form a rains form during Typhoon Mindulle. For Case 1, the infiltration rate of the slope surface is assumed follow the curve of the Horton infiltration equation, as shown in FIGURE 3a. While the rainfall intensity exceeds the curve, the values of the infiltration equation will be used as the input rainfall rate at that hour. To account for the surface drainage system on slope, which reduces infiltration, the rainfall intensities at each hour are assumed to be one-half (1/2) of the original rainfall. The infiltration rate, as shown in FIGURE 3b, is assumed for the rainfall input for Case 2 and 3.

4. An Example for the Simulation

The parameters for characterizing unsaturated water transport are available for Jiu-fen-er-shan (Lin et al, 2002). The parameters used are listed in TABLE 1 and were used to fit the empirical law of unsaturated water seepage proposed by van Genuchten (1980). The corresponding parameters for input in the finite difference FLAC program are tabulated in TABLE 2. The strength parameters and physical properties of the soil are estimated as in TABLE 3. Numerical infiltration simulations were performed for every hour of the assigned rainfall event for 36 hours. Pore pressures, saturations, and flow vectors were examined every 12 hours for the 36 hour duration.

5. Results and Discussion

The numerical analysis results of CASE 1 are detailed plotted in FIGURE 4 and 5. The initial steady state before applying rainfall should be reached to “mimic” the in-situ state of the slope including saturated groundwater flow and unsaturated flow. The initial saturation for unsaturated zone should be less than one as shown in FIGURE 4a. The flow vectors are also shown. The flow vectors in the saturated zone are much large than those in unsaturated zone. The initial negative pore pressures are distributed according to the van Genuchten empirical law as shown in FIGURE 5a above the groundwater level. The initial negative pore pressures can be up to -0.7e5 Pa. It is observed from FIGURE 4b~4d that the saturation gradually increases on the surface of the slope and the flow vectors gradually become larger. This means that the rainfall water is infiltrating into the slope. However, the flow is relatively slow due to the nature of slow

unsaturated water flow in the soil. From FIGURE 5b~5d, it can be seen that on crest of the slope, the negative pore pressures were reduced since the beginning of rainfall during the 36 hour rainfall. The negative pore pressures were reduced to about -0.2e5 Pa only. Disappearing of negative pore pressure due to saturation of the soil in a slope sometime causes a slope to become less stable.

After the rainfall simulations are carried out, the states of the numerical model at initial, 12, 24, 33 and 36 hours can be retrieved for calculation of safety factor for each cases (Case 1, 2 and 3). The factors of safety were plotted in FIGURE 6. It is shown that the factors of safety are reducing while the rainfall was still continuing. When the rainfall stopped 33 hours, the F.S. may increase back up at 36 hours.

The effect of rainfall infiltration is quite small for slopes with cracks filled; that is, if a slope has treated with erosion control and filling all the cracks, infiltration alone is unlikely to trigger a slope failure.

6. Conclusions

Numerical infiltration simulations were performed using FLAC code for a rainfall event during Typhoon Mindulle. Pore pressure, saturation, and flow vectors were examined for every 12 hours for 36 hours. From the numerically monitoring results it shows that the stability is better for slopes mitigated with the surface drainage system and toe drainage. It is also shown that rainfall infiltration into slope is slow and the infiltration effect is relatively minor due to slow water movement in unsaturated zones. If a slope has been treated with erosion control by filling all the cracks, infiltration alone is unlikely to trigger a failure.

References

1. FLAC User's Manual Version 5: *Fluid-Mechanical Interaction*. Itasca Consulting Group, Inc., Minneapolis, Minnesota, USA, 2005, pp. 2-1~2-53.
2. Lin, L.L., Ming, S., Lin, M.Y. and Tu, Y.T. Soil Water Characteristics for Jiu-fen-er-shan Landslide Area. (In Chinese.) *J. of Chinese Soil and Water Conservation*, Vol. 33, No. 2, 2002, pp.79-86.
3. van Genuchten, M. T. "A Closed-Form Equation for Predicting the Hydraulic Conductively of Unsaturated Soils". *Soil Sci. Soc. Am. J.*, Vol. 44, 1980, pp.892-898.
4. Abramson, L.W., Lee, T.S., Sharma, S. and Boyce, G..M. *Slope Stability and Stabilization Methods*, 2001, John Wiley & Sons, Inc., 736p.

TABLE 1 Parameters of the van Genuchten Empirical Laws for Jiu-fen-er-shan (Li et al, 2002)

Saturated hydraulic conductivity	Saturated water content	Residual water content	van Genuchten parameters	
K_s, (cm/hr)	θ_s, (cm^3/cm^3)	θ_r, (cm^3/cm^3)	α, (cm^{-1})	n
13.76	0.434	0.03165	0.01	1.5

TABLE 2 Corresponding Parameters Used in the Numerical Analysis for Jiu-fen-er-shan

FLAC parameters			Residual saturation	Capillary pressure, Pa	Saturated mobility coefficient, m^2/Pa-sec
a	b	c	S_r^w	P_0	k
0.333	0.5	0.5	0.083	9810	3.9e-9

Note: $\kappa_r^w = S_e^b[1-(1-S_e^{1/a})]$; $\kappa_r^g = (1-S_e)^c[1-S_e^{1/a}]^{2a}$; $a = 1-1/n$; $P_0 = \rho_w g/\alpha$;

$k = K_s/\rho_w g$; ρ_w = water density; g = gravity; κ_r^w = Permeability of "wetting" fluid (water)

κ_r^g = Permeability of "non-wetting" fluid (air/gas)

TABLE 3 Soil Parameters

Density	Bulk modulus	Shear modulus	Cohesion	Friction	Porosity
kg/m^3	Pa	Pa	Pa	deg	
1310	2.67e7	1.67e7	0	35	0.5

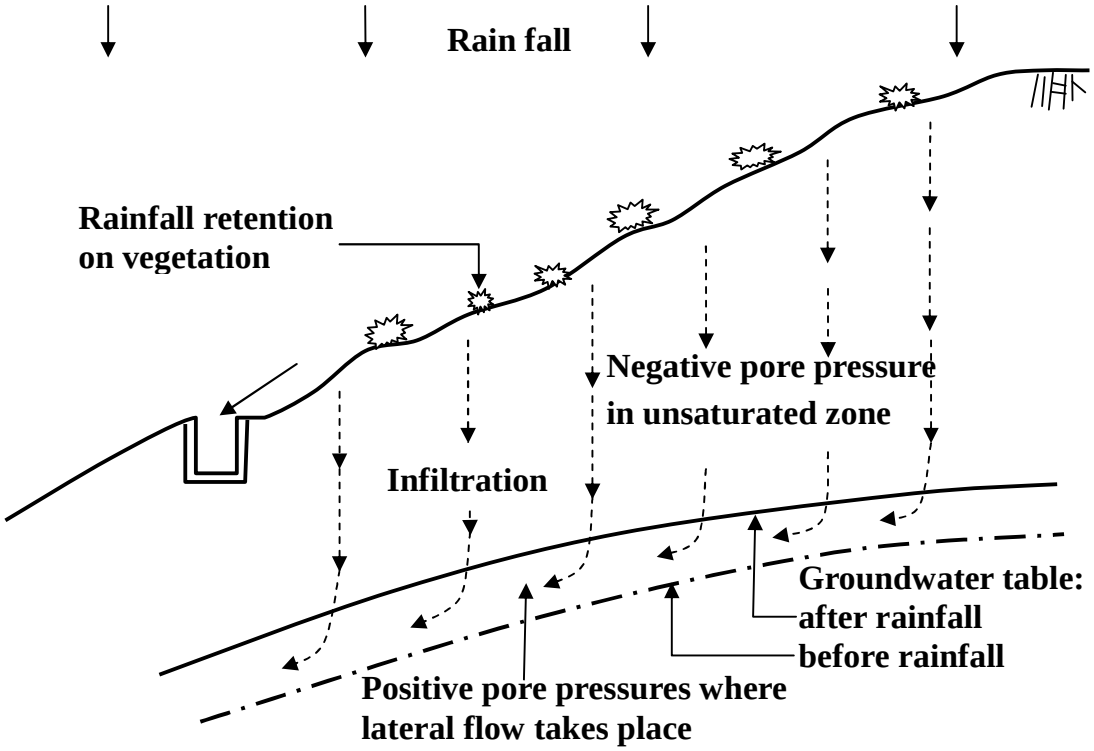

FIGURE 1 Infiltration into a slope and a possible groundwater table after rainfall (modified form Abramson et al., 2002)

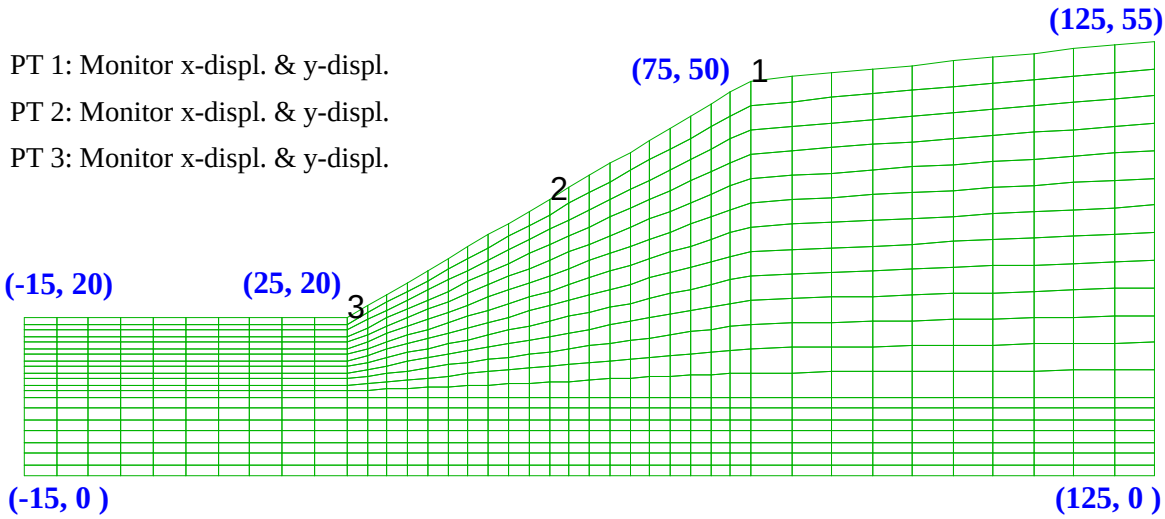

FIGURE 2 The finite difference mesh used in FLAC and the numerical monitored Points 1, 2 and 3

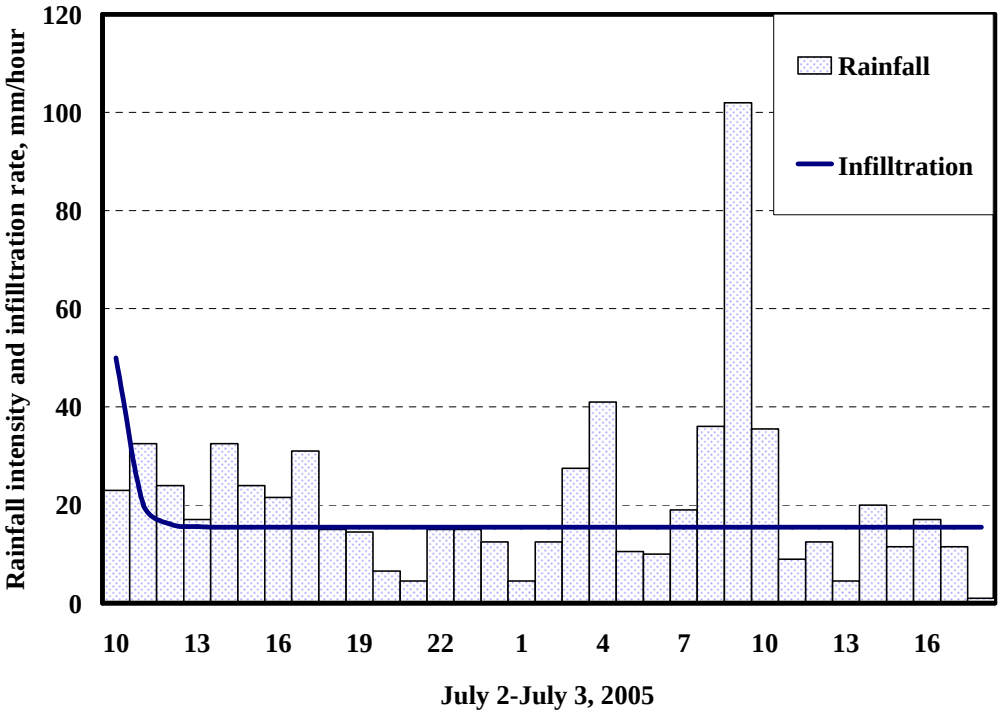

FIGURE 3a Rainfall and infiltration rate for Case 1.

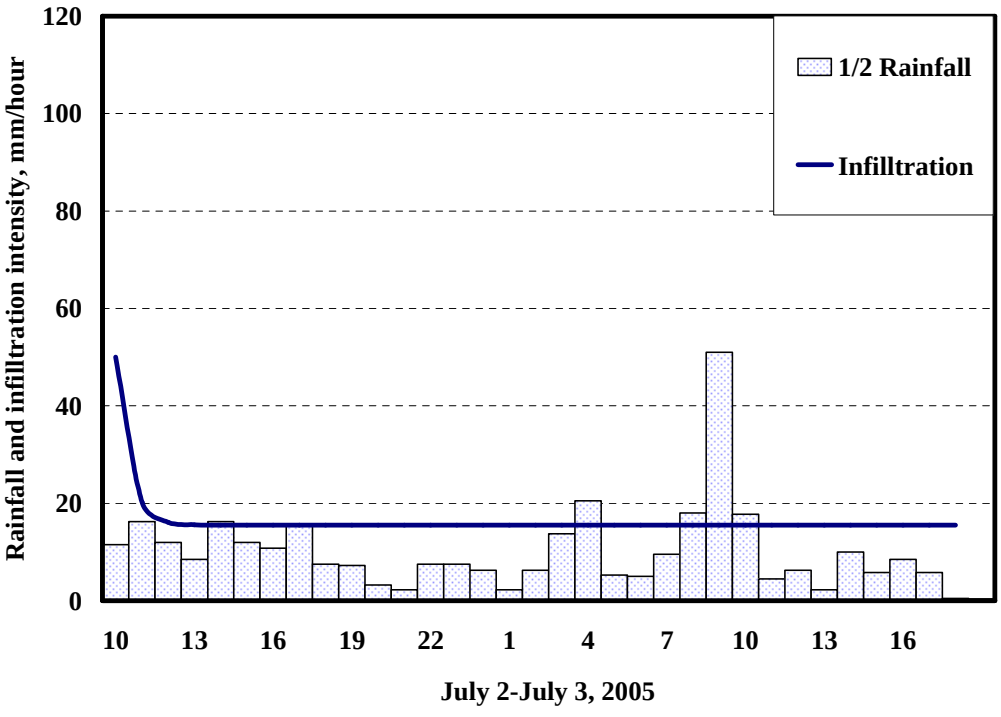

FIGURE 3b One-half rainfall and infiltration rate for Case 2 and 3.

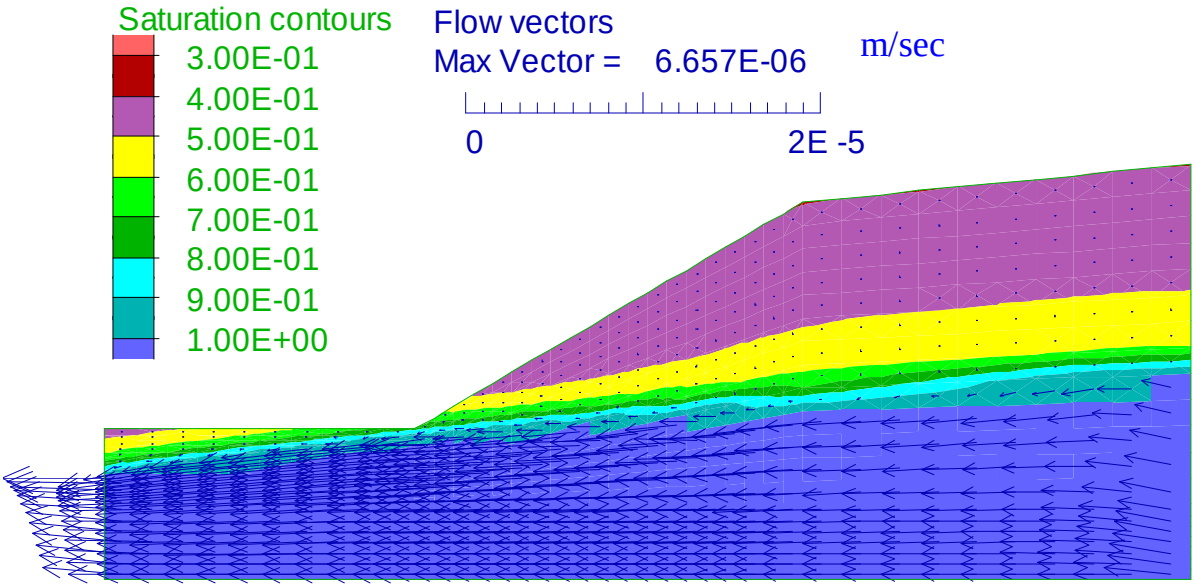

FIGURE 4a The initial steady state saturation and the flow vectors (Case 1).

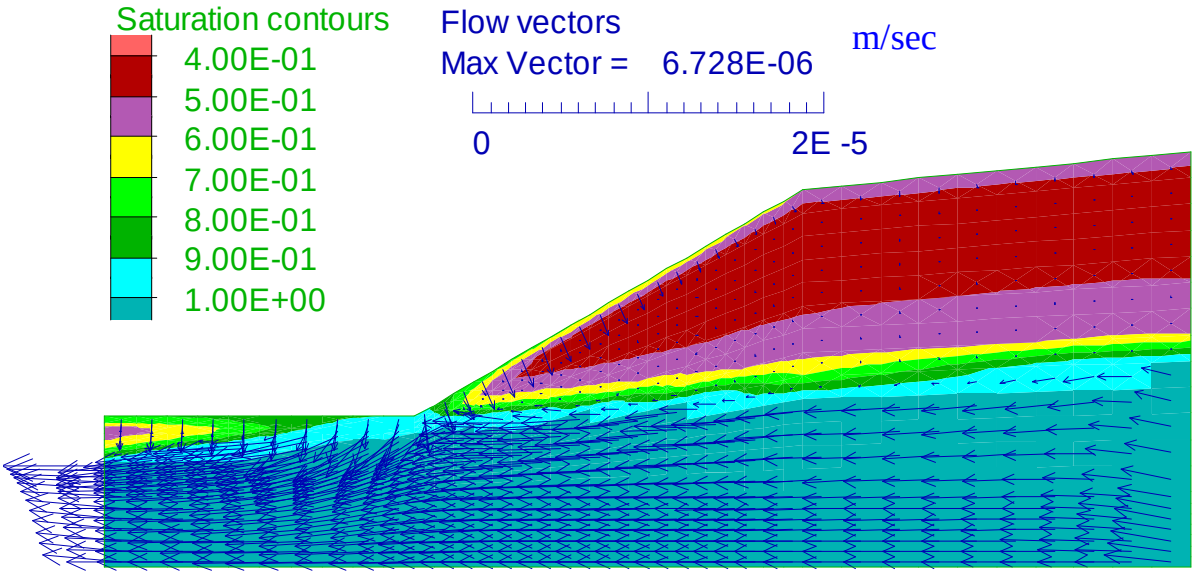

FIGURE 4b The saturation contours and the flow vectors at 12hr(Case 1).

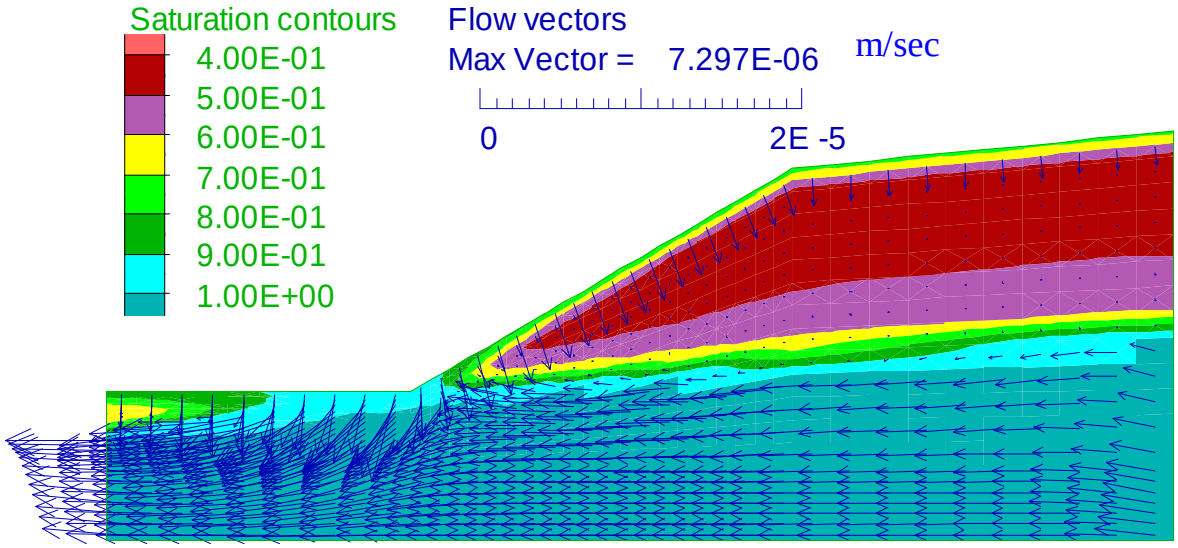

FIGURE 4c The saturation contours and the flow vectors at 24hr(Case 1).

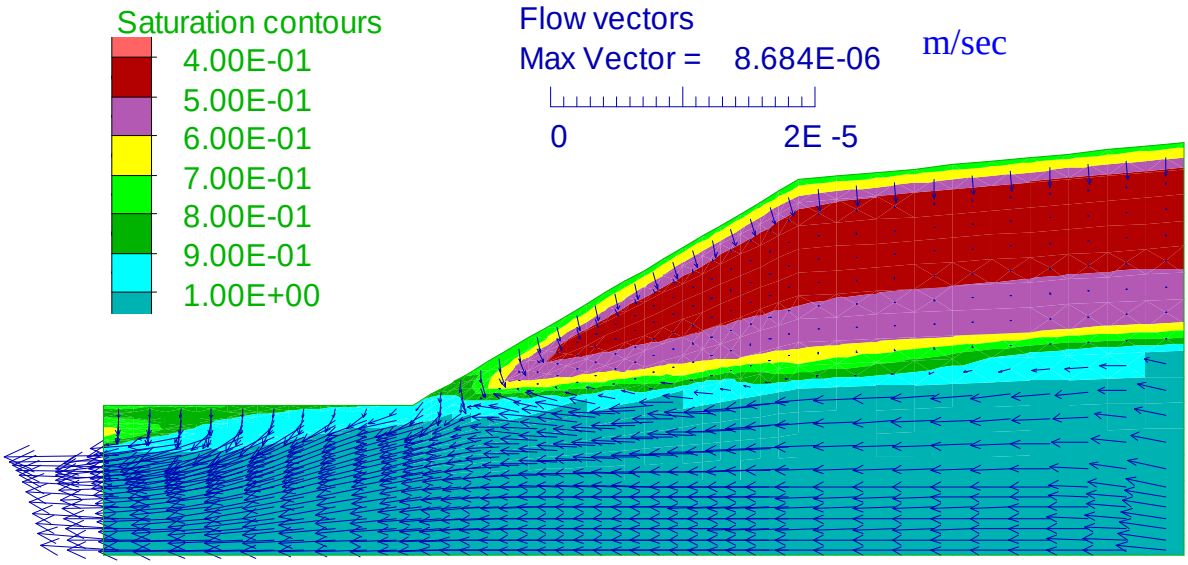

FIGURE 4d The saturation contours and the flow vectors at 36hr(Case 1)

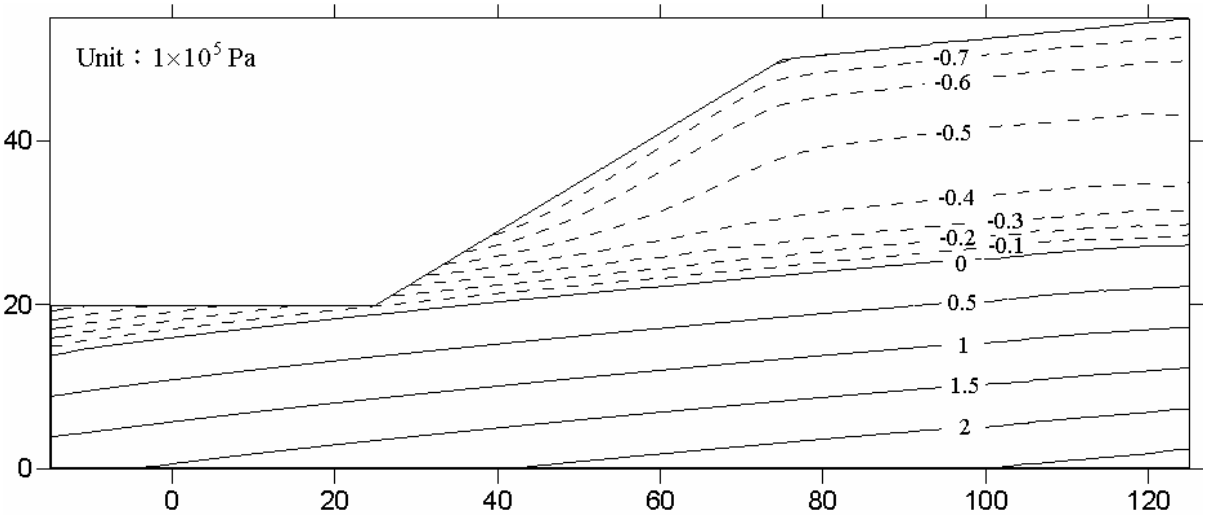

FIGURE 5aThe initial pore pressure contours(Case 1).

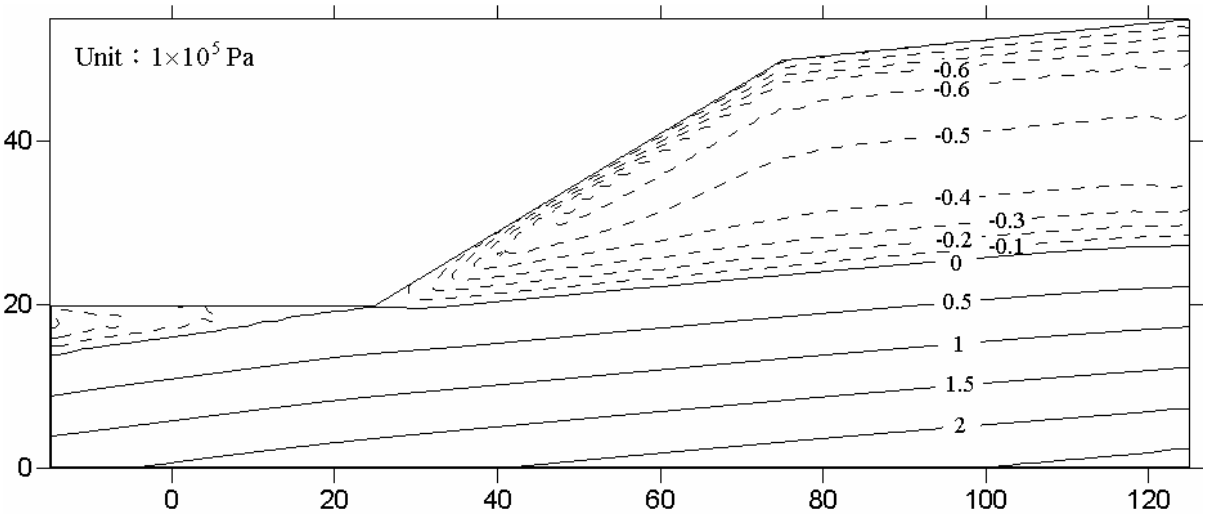

FIGURE 5b The pore pressure contours at 12 hr(Case 1).

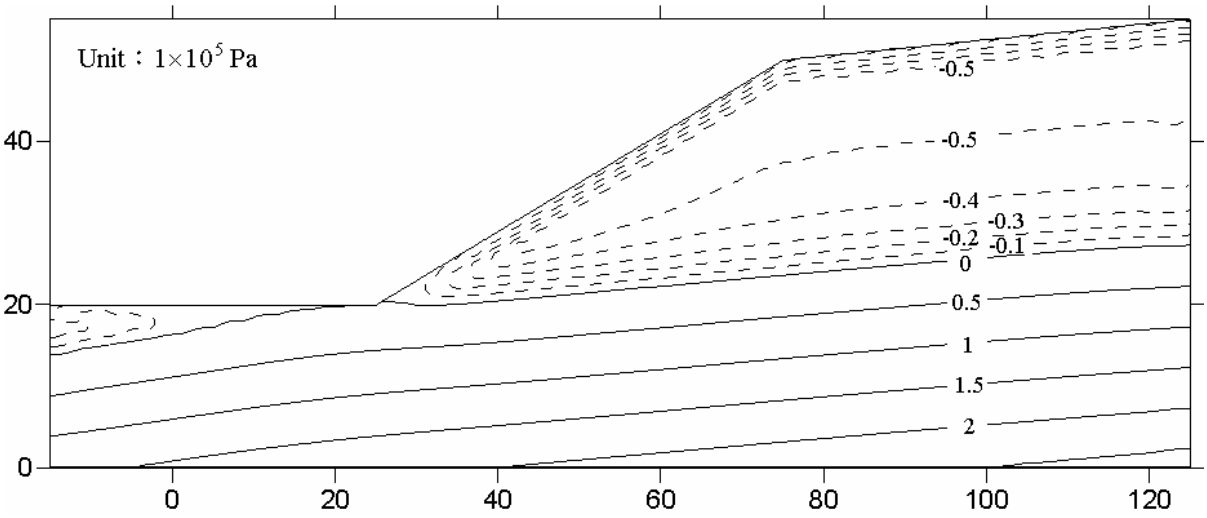

FIGURE 5c The pore pressure contours at 24 hr(Case 1).

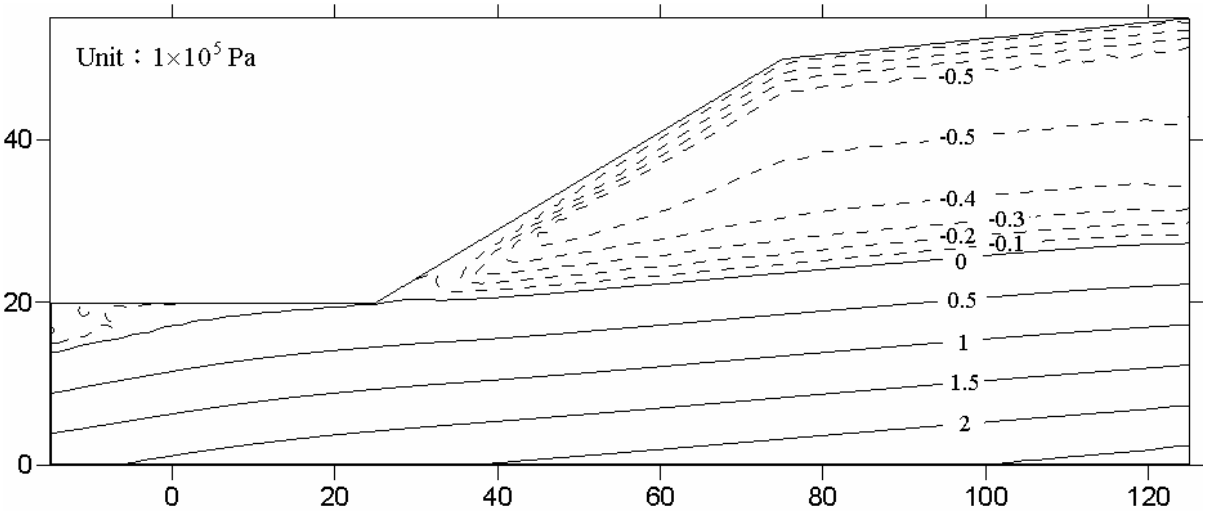

FIGURE 5d The pore pressure contours at 36 hr(Case 1).

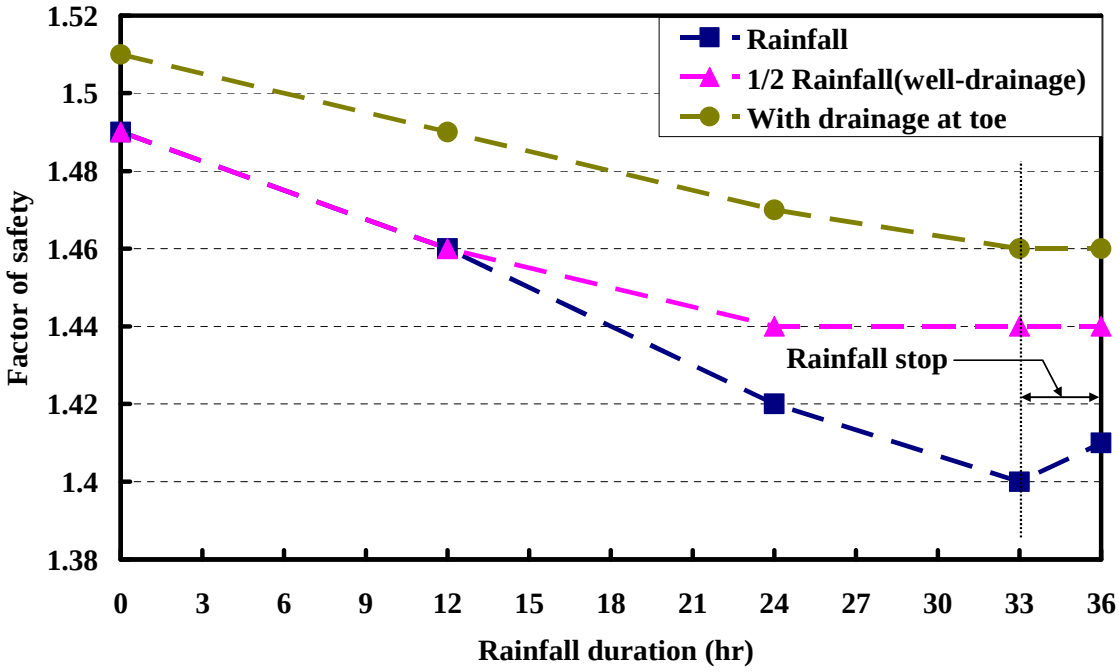

Figure 6 Factor of safety for Case 1, 2 & 3